# An assessment of Backward and Forward Euler methods applied to the Prandtl problem

F.B. Mok and D.V. Griffiths

Department of Engineering, University of Manchetser

## INTRODUCTION

The limit load of a soil mass can be determined numerically by the finite element method which remains one of the most versatile approaches for analysing geotechnical problems. In the past two decades, various strategies have been proposed for integrating the elasto-plastic rate equation. Various iso-error maps have been produced so as to compare the accuracy of these methods. In this paper, some of these methods are applied to the Prandtl problem and their accuracy and efficiency compared.

The details of the mesh are shown in Figure 1. It consists of 8-node quadratic plane strain elements. The element matrices are formed by using reduced integration. An elastic, perfectly-plastic material is assumed. Two different yield criteria are used; namely von Mises and Mohr-Coulomb with $\phi$=0. An 'initial stress' approach is used and all the iterations employed a constant global stiffness matrix, hence, a modified Newton Raphson method. The limit load of the footing is $(\pi+2)C_u$. Since the main emphasis is on the rate integration algorithms, the adequacy of the mesh has not been considered.

The mesh had been analysed by the 'viscoplastic' approach found in Reference 1, which ensures that global equilibrium is achieved. However, the various integration algorithms studied in this paper will also maintain the consistency requirement, hence all the Gauss-points are kept near to the yield surface within a tight tolerance. As a result, the solutions as well as the computational effort are different from Reference 1.

In all the elasto-plastic integrations, an incremental elastic stress is predicted. If the resultant stress causes yielding to occur, a 'plastic' stress is applied to bring the resultant stress back to the yield surface, i.e., to ensure the consistency requirement is met. The position at which the plastic stress is evaluated depends on the algorithm used and ultimately, affects the solution obtained.

## METHODS OF INTEGRATING THE ELASTO-PLASTIC RATE EQUATION

### Preliminary

In all the subsequent discussion, $\sigma_x$ refers to the unyielded stress at the start of a step, $\Delta\sigma_e$ is the incremental stress, $\sigma_A$ is the contact stress at which yield occurs and $\sigma_B$ is the stress obtained if wholly elastic response is postulated, i.e., 'the trial stress'. The final stress is denoted as $\sigma_C$ (Figure 2). **a** is the flow vector and occurs when the material is yielded (i.e., $a_A$, $a_B$ only $a_C$). $f_X$, $f_A$, $f_B$ and

$f_C$ are the values of the yield function.

Oritz and Popov[2] have shown that a number of the elasto-plastic integration algorithms can be represented in the generalised form:

$$\sigma_C=\sigma_A+\mathbf{D}(\Delta\varepsilon-\Delta\varepsilon_p)$$

where $\Delta\varepsilon_p=\Delta\lambda[(1-\theta)\mathbf{a}_A+\theta\mathbf{a}_C]$

or $\Delta\varepsilon_p=\Delta\lambda[\mathbf{a}((1-\theta)\sigma_A+\theta\sigma_C)]$ $\quad 0\le\theta\le1$

$\Delta\varepsilon$ and $\Delta\varepsilon_p$ are the incremental total and plastic strains and $\Delta\lambda$ is the plastic strain rate multiplier, **D** is the stress and strain matrix.

(a) Forward Euler method

In this method[3] ($\theta=0$), the plastic stress is evaluated at the point where contact of the yield surface occurs (Figure 2). The contact stress, $\sigma_A$, is found by solving the equation $f(\sigma_x+\alpha\Delta\sigma_e)=0$ with $(0\le\alpha\le1)$.

In most cases, the contact point can be determined by iteration. In an elastic-perfectly plastic material, its evaluation is made simpler as the yield surface does not change in size. An explicit relation between the yield function f and $\alpha$ can be written for a von Mises material. Similarly, a linear interpolation between $f_X$ and $f_B$ is sufficient to determine $\alpha$ in a Mohr-Coulomb material, Appendix 1.

Hence, the increase in stress is,

$$\Delta\sigma=\mathbf{D}\Delta\varepsilon-\Delta\lambda\mathbf{D}\mathbf{a}_A$$

$$=\Delta\sigma_e-\Delta\lambda\mathbf{D}\mathbf{a}_A, \qquad \text{where } \Delta\lambda=\frac{\mathbf{a}_A{}^T\mathbf{D}\Delta\varepsilon}{\mathbf{a}_A{}^T\mathbf{D}\mathbf{a}_A}$$

The final stress is, $\sigma_C=\sigma_X+\alpha\mathbf{D}\Delta\varepsilon-(1-\alpha)\Delta\lambda\mathbf{D}\mathbf{a}_A$

Even though small load steps are used, the consistency requirement may not be met at convergence. This always results in 'drift' from the yield surface[4]. If not corrected, too high a limit load or too stiff a response is predicted. The 'drift' can be corrected along the normal of the yield surface or along the radial of the deviatoric plane as in the von Mises material.

Another way to reduce the drift and obtain a better solution is to sub-increment the elastic stress[4]. With a sufficient number of sub-increments, the drift correction is not necessary. However, it is difficult to determine the number of required sub-increments in advance. Sloan[5] used a two step Euler forward procedure to estimate the error produced and hence to compute the required number of sub-increments. In this paper, an empirical relationship is used to determine the number of sub-

increments. It is expressed in a Fortran statement: ISTEP=INT(20*$\frac{f_B}{\sigma_o}$+1) where $\sigma_o$ is the yield stress. Clearly, the number of sub-increments depends on the size of the yield surface.

(b) Backward Euler method

An alternate position to work out the corrector stress is at point B (Figure 2) by putting $\theta$=1 and avoids the necessity of computing the intersection point A. For an elastic perfectly plastic material, the yield function is linearised around the current values of the state variables[6] to obtain:

$$f=f_B+\frac{\delta f^T}{\delta \sigma}\Delta\sigma$$

$$=f_B-\Delta\lambda a_B{}^T D a_B, \qquad \text{where } \Delta\lambda=\frac{f_B}{a_B{}^T D a_B}$$

The increase in stress is, $\Delta\sigma=\Delta\sigma_e-\frac{f_B D a_B}{a_B{}^T D a_B}$

In general plasticity, the state variables which defined the current size of the yield surface have to be included. The corrected stress will not lie on the yield surface at the trial contact point, iterations are required to meet the consistency requirement (the closest point algorithm).

The final stress at convergence will not always lie on the yield surface and corrections used in the forward method are similarly applied. However, that is not required for a von Mises material with non-hardening under 3-D stress state as the method coincides with the 'radial return algorithm'.

In the deviatoric plane, all the stress components can be represented by concentric circles for a von Mises material under 3-D stress state, Figure 2. As a result, point C can be determined by the radial joining point B and the axes origin on the deviatoric plane.

$$\sigma_C=r\sigma_B, \qquad \text{where } r=\frac{\sigma_o}{f_B+\sigma_o}, \qquad 0\le r\le 1$$

Rice and Tracey[7] suggested the mean normal method for a von Mises material with rigid hardening. The average value of the contact stress $\sigma_A$ and trial stress $\sigma_B$ is taken and the consistency requirement results in $\frac{(a_A+a_B)^T\Delta\sigma}{2}=0$.

In a von Mises material with perfect plasticity and under 3-D stress state, this procedure ensures the final stress lies on the yield surface and no Gauss-point level iterations are required.

## RESULTS

The load-deflection curves are shown in Figures 3 and 4 whereas the number of iterations are detailed in Tables 1 and 2. The forward Euler method predicts a higher limit load and surprisingly,

more total number of iterations. A more satisfying solution is obtained when sub-incrementation is used. Another analysis (which is not shown) uses 10 equal sub-increments and the results are identical to the one presented here. If only 3 sub-increments are used, not much improvement in the solution is gained. All the backward methods produce (almost) identical results and the total number of iterations are less than the forward method. In column 3 and 5, the bracketed values represent the analyses with which a certain amount of the bodyloads are carried forward to the next load step. The magnitude depends on the ratio of the sizes of the load step. In some steps, the amount of iterations is reduced by a half.

In another series of analyses (Figure 3b), the size of the load steps is doubled. Again, the superiority of the backward methods and the importance of sub-incrementation are shown. Whereas a stiff response is predicted by the forward method, the others evaluate an acceptable limit load. Moreover, the deflections obtained at the intermediate steps (and final one) are similar to the previous series of analyses.

The analyses are then carried on by using a Mohr-Coulomb yield criterion (with $\phi$=0). Similar observations can be made (Figure 4). To eliminate numerical problems, a higher Poisson ratio of 0.4 is used with this series of analyses.

## CONCLUSIONS

Small load steps are always recommended in elasto-plastic analyses to achieve convergent solutions. It appears that it is not a stringent requirement to follow. Convergence depends on the numerical procedure used and moreover, the consistency requirement must be enforced at each Gauss point. In this paper, a simple yield surface is used which results in simpler implementation of the backward algorithms. In general plasticity, however, the rate of the flow vector is required (which may not be possible to obtain) in which case, forward methods may be preferred with sub-increments. An empirical relationship has been used to find out the number of sub-increments in an elastic and non-hardening plastic material and proved to yield acceptable results.

The implementation of the above algorithms into a hyperbolic soil model is being carried out and will be reported when the results are available. Recently, work in which the stiffness is updated at each iteration, i.e., the full Newton Raphson approach, attention has been focused on determining a 'consistent' stiffness matrix[8] as opposed to the standard matrix so as to maintain a quadratic convergence rate of the solution. The standard method has been tried but more effort is required to implement the former. It is hoped to publish the results in the near future.

"Software Engineering"



APPENDIX 1

For a von Mises material in plane strain, $\alpha$ can be obtained from the expression[9]:

$$\alpha=\frac{-3b\pm\sqrt{9b^2-12a(3c-\sigma_o^2)}}{6a}$$

where $a=\frac{1}{2}(\Delta s_{xe}^2+\Delta s_{ye}^2+\Delta s_{ze}^2)+\Delta\tau_{xye}^2$

$$b=s_x\Delta s_{xe}+s_y\Delta s_{ye}+s_z\Delta s_{ze}+2\tau_{xy}\Delta\tau_{xye}$$

$$c=\frac{1}{2}(s_x^2+s_y^2+s_z^2)+\tau_{xy}^2$$

$s_x$, $s_y$ and $s_z$ are the deviatoric stress components.

(Only the positive value of $\alpha$ from the above equation is used.)

For a Mohr-Coulomb material in plane strain, $\alpha$ is determined from a linear interpolation of $f_X$ and $f_B$ to yield an accurate contact stress,

$$\alpha=\frac{f_B}{f_B-f_X}$$

REFERENCE

(1) Smith, I.M. & Griffiths, D.V., *Programming the finite element method*, John Wiley & Sons (1988)

(2) Oritz, M. & Popov E.P., Accuracy and stability of integration algorithms for elasto-plastic constitutive relations, *Int. J. Num. Meth. Engg.*, **21**, 1561-1576 (1985)

(3) Crisfield, M.A., *Non-linear finite element analysis of solids and structures, Volume 1: Essentials*, John Wiley & Sons (1991)

(4) Nayak, G.C. & Zienkiewicz, O.C., Elasto-plastic stress analyses. A generalization for various constitutive relations including strain softening, *Int. J. Num. Meth. Engg.*, **5**, 113-135 (1972)

(5) Sloan, S.W., Substepping schemes for the numerical integration of elasto-plastic stress-strain relations, *Int. J. Num. Meth. Engg.*, **24**, 893-912 (1987)

(6) Oritz, M. & Simo, J.C., An analysis of a new class of integration algorithms for elasto-plastic constitutive relations, *Int. J. Num. Meth. Engg.*, **23**, 353-366 (1986)

(7) Rice, J.R. & Tracey, D.M., Computation fracture mechanics, *Proc. Symp. Num. Meth. Struct. Mech.*, ed. S.J. Fenves, Academic Press (1973)

(8) Simo. J.C. & Taylor, R.L., Consistent tangent operators for rate-independent elasto-plasticity, *Comp. Meth. Applied Mech. Engg.*, **48**, 101-118 (1985)

(9) Bicanic, N.P., Exact evaluation of contact stress in computational elasto-plasticity, *Engg. Comp.*, **6**, 67-73 (1989)

| Load ($kN/m^2$) | from Reference 1 | Forward-Euler method | Forward-Euler method with sub-increments | Mean Normal method | Backward-Euler method | Radial Return method |
|---|---|---|---|---|---|---|
| 200 | 2 | 2 (2) | 2 | 2 | 2 (2) | 2 |
| 300 | 19 | 19 (10) | 20 | 20 | 20 (20) | 20 |
| 350 | 29 | 29 (27) | 39 | 39 | 43 (41) | 43 |
| 400 | 47 | 46 (36) | 59 | 60 | 64 (49) | 64 |
| 450 | 67 | 64 (49) | 78 | 78 | 83 (60) | 83 |
| 480 | 91 | 82 (57) | 109 | 111 | 116 (84) | 116 |
| 500 | 100 | 104 (66) | 130 | 132 | 136 (85) | 136 |
| 510 | 115 | 113 (55) | 144 | 148 | 150 (79) | 150 |
| 515 | 145 | 126 (64) | 157 | 161 | 166 (80) | 166 |
| 520 | 250 | 136 (52) | 250 | 250 | 250 (250) | 250 |
| 525 | | 152 (45) | | | | |
| 530 | | 223 (124) | | | | |
| 535 | | 250 (250) | | | | |

Table 1a Number of iterations required with small load steps (von Mises material).

| Load ($kN/m^2$) | from Reference 1 | Forward-Euler method | Forward-Euler method with sub-increments | Mean Normal method | Backward-Euler method | Radial Return method |
|---|---|---|---|---|---|---|
| 200 | 2 | 2 | 2 | 2 | 2 | 2 |
| 400 | 32 | 32 | 58 | 57 | 60 | 60 |
| 500 | 53 | 53 | 130 | 123 | 138 | 138 |
| 510 | 250 | 65 | 144 | 148 | 145 | 145 |
| 520 | | 79 | 250 | 250 | 250 | 250 |
| 525 | | 94 | | | | |
| 530 | | 110 | | | | |
| 535 | | 119 | | | | |
| 540 | | 125 | | | | |
| 545 | | 142 | | | | |

Table 1b Number of iterations required with large load steps (von Mises material).

| Load ($kN/m^2$) | Forward-Euler method | Forward-Euler method with sub-increments | Backward-Euler method |
|---|---|---|---|
| 200 | 2 | 2 | 2 |
| 300 | 15 | 15 | 16 |
| 350 | 34 | 36 | 37 |
| 400 | 48 | 55 | 58 |
| 450 | 61 | 69 | 73 |
| 480 | 88 | 100 | 104 |
| 500 | 104 | 113 | 121 |
| 510 | 118 | 124 | 127 |
| 515 | 122 | 143 | 147 |
| 520 | 141 | 250 | 250 |
| 525 | 250 | | |

Table 2a Number of iterations required with small load steps (Mohr-Coulomb material).

| Load ($kN/m^2$) | Forward-Euler method | Forward-Euler method with sub-increments | Backward-Euler method |
|---|---|---|---|
| 200 | 2 | 2 | 2 |
| 400 | 44 | 52 | 52 |
| 500 | 80 | 120 | 124 |
| 510 | 106 | 124 | 128 |
| 515 | 118 | 144 | 146 |
| 520 | 123 | 250 | 250 |
| 525 | 136 | | |
| 530 | 170 | | |
| 535 | 250 | | |

Table 2b Number of iterations required with large load steps (Mohr-Coulomb material).

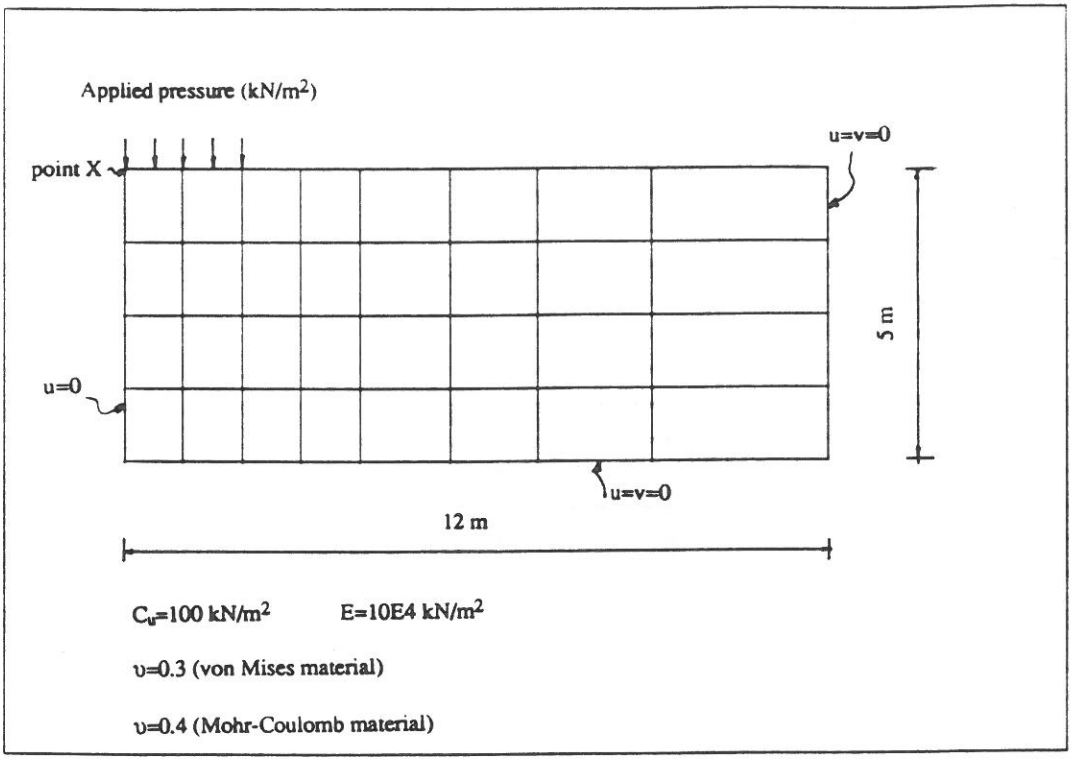


Figure 1 Details of the finite element mesh

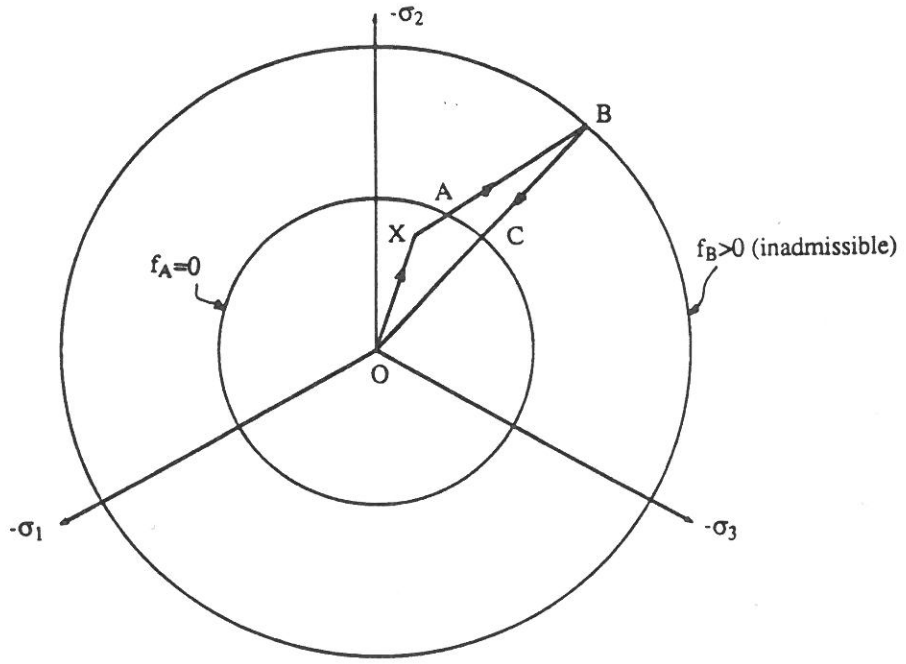


Figure 2 Various locations for the integration of an elastic perfectly plastic von Mises material shown on the deviatoric plane

Figure 3 Load deflection curves at point X for a von Mises material

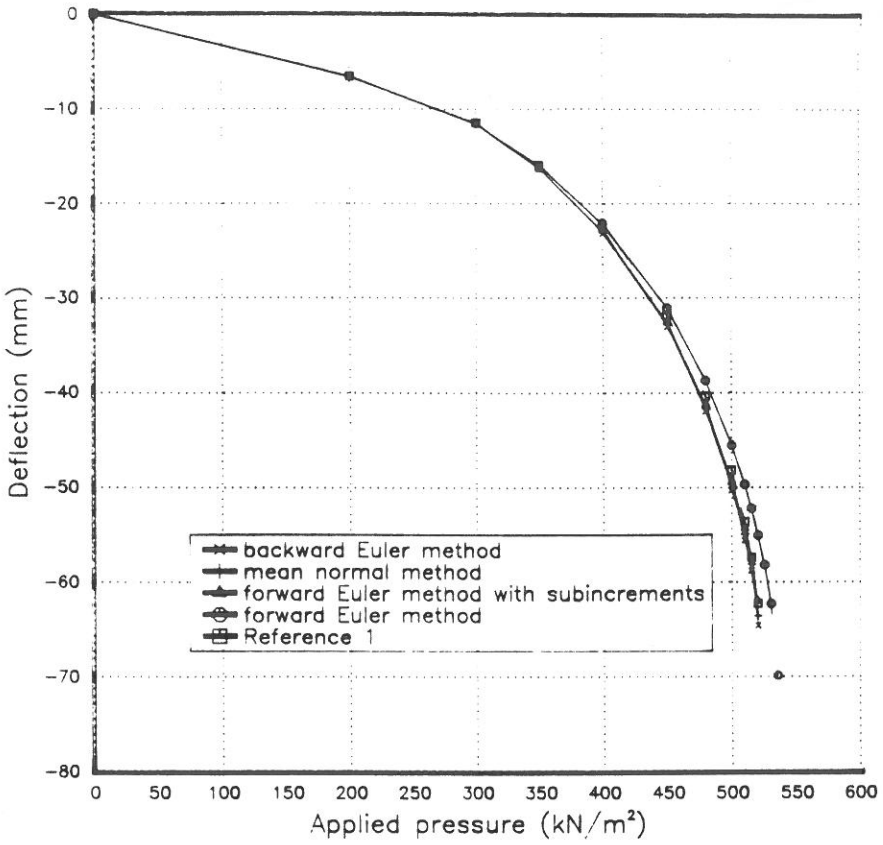


(3a) Small load steps

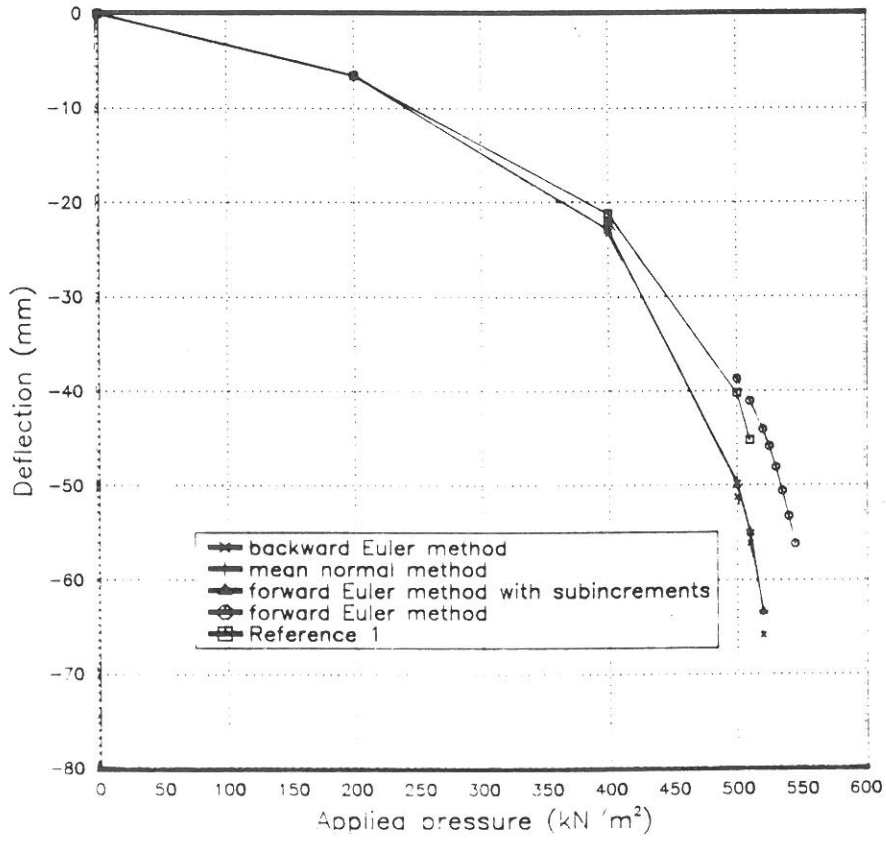

Figure 4 Load deflection curves at point X for a Mohr–Coulomb material

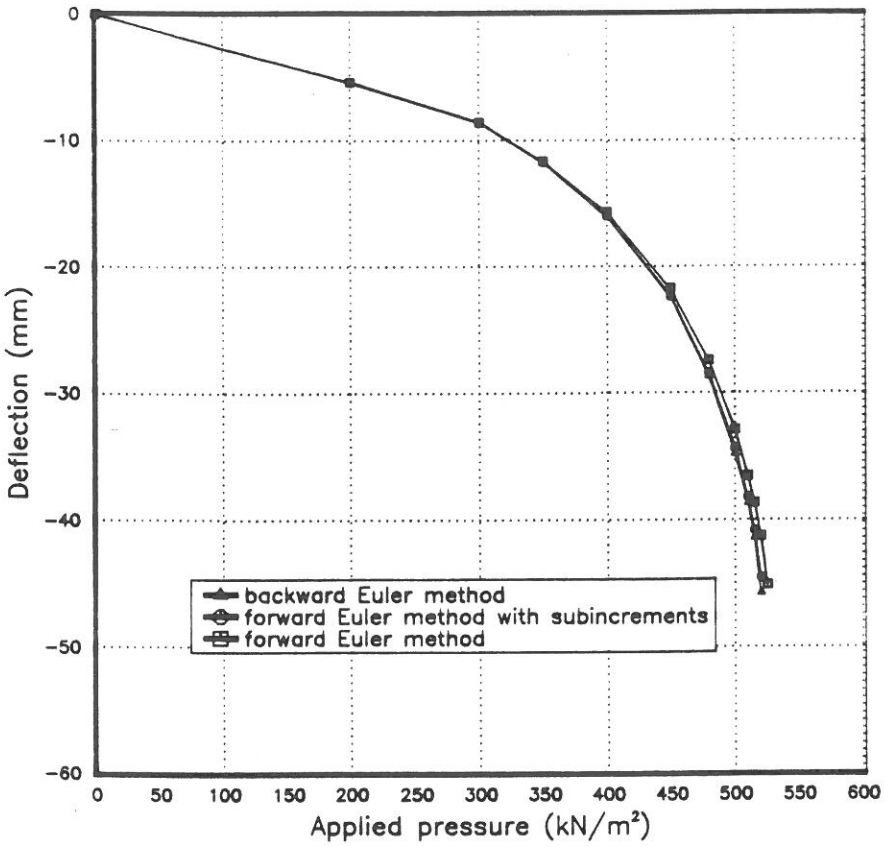


(4a) Small load steps

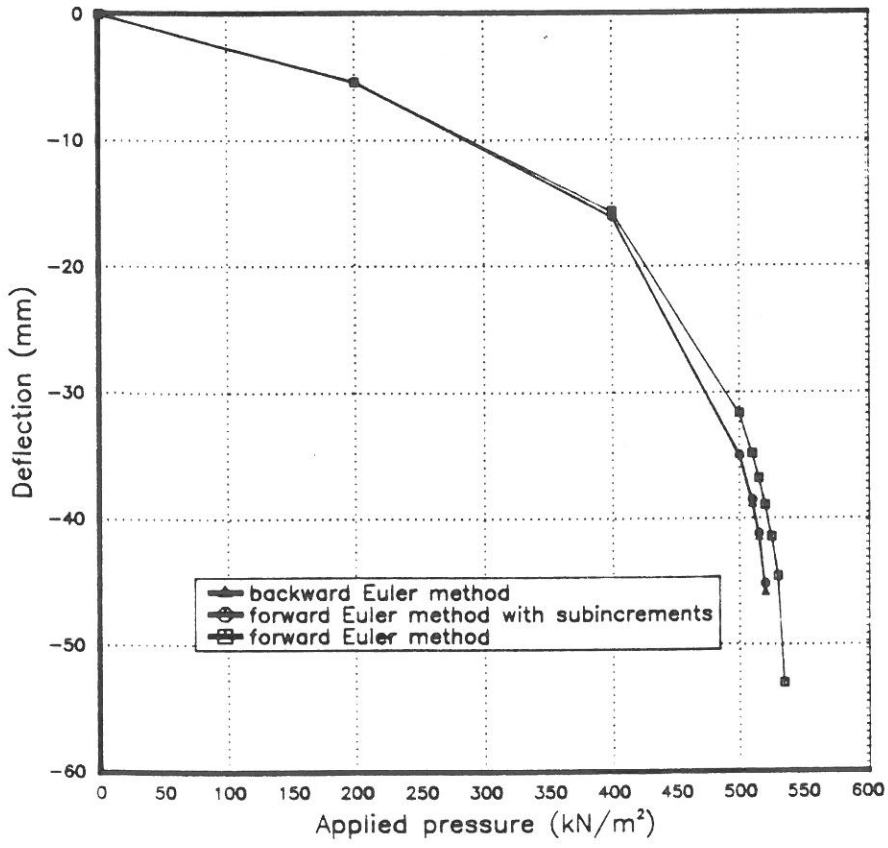


(4b) Large load steps